An Optimal Energy Management System for Marine Hybrid Power Systems

Daeseong Park
Dept. of Marine Technology
Norwegian University of Science and Technology
Trondheim, Norway
daeseong.park@ntnu.no

Florian Perabo
Dept. of Marine Technology
Norwegian University of Science and Technology
Trondheim, Norway
florian.perabo@ntnu.no

Minjoo Choi
Dept. of Naval Architecture and Ocean Systems Engineering
Korea Maritime and Ocean University
Busan, Republic of Korea
minjoo.choi@g.kmou.ac.kr

Espen Skjong
Research, Development and Technology
Blue Ctrl AS
Ålesund, Norway
espen.skjong@bluectrl.io

Mehdi Zadeh
Dept. of Marine Technology
Norwegian University of Science and Technology
Trondheim, Norway
mehdi.zadeh@ntnu.no

***Abstract*—This paper proposes an optimal control strategy for the energy management system (EMS) of marine hybrid power systems with the objective of reducing operational expenses (OPEX) and environmental emissions. Here, the OPEX includes main parameters such as the fuel consumption, degradation, and maintenance of diesel engines. The engines as the maintenance-intense devices in the power systems are expensive to operate not only due to the fuel cost, but also the cost of maintenance and overhaul. Hence, better engine management will improve the overall system efficiency and reliability. In the proposed method, the engine operation is further improved in terms of running hours and transient loading. The optimization algorithm is designed based on mixed-integer linear programming (MILP) considering the physical constraints of the engine-generators and battery-related limits. The developed EMS is then tested with a real ship profile by the different cases of with and without battery and with various battery capacities. The results show the effectiveness of the proposed EMS to improve the operation of the hybrid power system for a stable, efficient, and reliable ship operation.**

***Index Terms*—Marine power system, energy management, energy storage system, optimization, mixed-integer linear programming (MILP)**

I. Introduction

To meet the increasingly strict emission and efficiency requirements set by International Maritime Organization (IMO), the maritime industry must undergo a transition to low- and zero-carbon technologies. In this light, the extensive electrification and hybridization of ships have become a major technology trend, thus increasing the efficiency, performance, and flexibility of ship power systems (SPS) [1], [2]. Energy storage systems (ESS) such as batteries provide benefits to the power system in terms of increased system stability and efficiency as well as reduced operational costs [3], [4].

In the hybrid power systems, the engines compensate for the energy deficit of the ESS, while the ESS facilitates optimal loading of the engines. Fig. 1 shows typical topologies of hybrid power systems including the placement of the ESS. In AC-based power systems, the ESS is usually connected to the main AC bus by a DC/AC converter in Fig. 1(a) or integrated into the DC-link of the propulsion motor drives by a DC/DC converter in Fig. 1(b). In DC hybrid power systems, the ESS is connected to the main DC bus by a DC/DC converter in Fig. 1(c). The DC/DC converters can be omitted if the voltage of the ESS and the DC bus are within a similar range. This approach reduces installation costs but prohibits the direct control of the ESS.

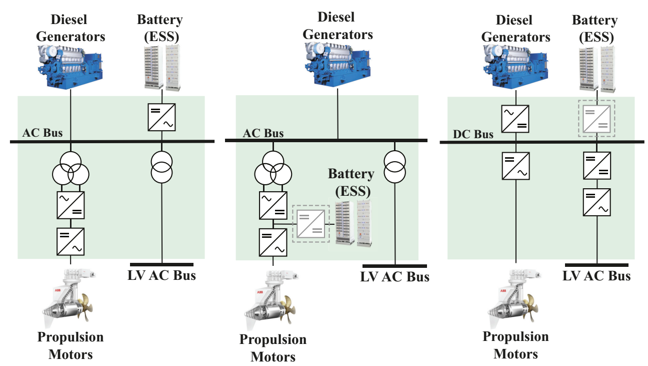

(a) AC Bus (opt1) (b) AC Bus (opt2) (c) DC Bus

Fig. 1: Battery integration strategies for shipboard AC and DC power systems

Hybrid electric ships show increased energy efficiency, reliability, and power system redundancy as well as reduced fuel consumption and emissions [5]. However, to utilize this great potential, advanced control strategies are crucial. While the power management system (PMS) ensures the availability of sufficient power and coordinates/limits heavy consumers at every time instant, the energy management system (EMS) is a higher-level control optimizing the energy efficiency, system reliability, and lifetime of ESSs [1]. Rule-based EMS represents a straightforward high-level control with sufficiently good results, but with the increasing complexity of hybrid power systems and uncertain system conditions, the formulation of rules becomes difficult, and the results tend to be sub-optimal [6]. Examples of rule-based EMS can be found in [2], [7], [8].

Alternative approaches are optimization-based control schemes using global planning and real-time optimization methods. Generally, the optimization problem is formulated as the minimization of a constrained cost function considering technical and economic concerns [6], such as diesel engine's optimal operating point based on specific fuel consumption curve [9], total fuel cost, maintenance cost represented as running time of the plant, system efficiency and battery ageing. Global optimization approaches include classical optimization methods such as linear/nonlinear programming (LP/NLP) [10], mixed-integer linear/nonlinear programming (MILP/MINLP) [11], [12] and dynamic programming (DP) [13] as well as heuristic methods such as particle swarm optimization [6] and genetic algorithms [14]. Commonly used real-time methods include model predictive control (MPC) [15] and equivalent consumption minimization strategy (ECMS) [2]. Further examples of optimization-based EMS can be found in [16].

Due to the nonlinearity and complexity of SPS, LP has been rarely used although it is a simple and fast optimization method [16] mainly because of the fuel consumption calculation. When the EMS is formulated with nonlinear functions, the application of online optimization becomes difficult due to the calculation burden. Then, this optimization-based EMS can be only used as an offline optimization that plans a ship operation with a predicted load profile before the ship starts to sail. As a result, offline optimization cannot produce accurate performance due to many uncertainties, while online optimization can use the actual power system state measurements.

The main burden towards the use of online optimization is to formulate the fuel consumption for marine engines. The fuel consumption can be calculated based on a specific fuel consumption (SFC) curve which is usually given by the engine manufacturer. But, the SFC curve is a nonlinear function with a large variation from no-load to full-load operation. This requires the inclusion of nonlinear functions in the optimization problem so that the algorithm should calculate gradients to find the next directions and repeat this process until the optimal solution has been found. If the objective problem can be formulated as LP, the solver can check the corner points to find the optimal point with comparatively less calculation time and effort. Furthermore, the LP solvers are more welcomed in practical applications. Hence, converting the SFC into a piecewise linear function can help the optimization-based EMS to be applied in the real application.

Considering an EMS, some control quantities such as the number of running gensets, the number of genset starts/stops, and switching states can be represented by integers and binaries. MILP and MINLP consider both restricted and unrestricted quantities which makes these approaches more appropriate for EMS optimization problems than LP. A MILP algorithm-based EMS for three different diesel-electric power system configurations (fixed-speed, variable-speed, and ESS integration) is used in [11] showing reduced fuel consumption and genset operating hours compared to a rule-based algorithm. In [12], the optimal sizing of an ESS for a ship hybrid power system is calculated based on the optimization results of an EMS using MILP. A numerical optimization based on the efficiency model of a hybrid power system is presented in [5]. The algorithm calculates the optimal loading conditions and decides whether the generators are operated continuously or periodically charge/discharge the battery. Also, an online optimization strategy is implemented comparing the efficiency of different operational modes. However, for such a hybrid power system, the optimization problem should include a range of variables from fuel consumption to the degradation and maintenance of the engines.

In this paper, an optimal energy management system (EMS) algorithm is proposed for shipboard hybrid power systems with engines and marine batteries. The proposed EMS includes an online optimization algorithm to reduce the OPEX of the ship operation such as the fuel consumption and other costs related to maintenance of engines. The optimization algorithm utilizes a SFC curve as a piecewise linear function to calculate the fuel consumption in the objective function so that the optimization problem can remain in the form of an LP with mixed integers (MILP). Besides that, to convert absolute functions for penalizing terms in the objective function, the goal programming approach is used to keep the linear form as well. The proposed method also considers the constraints such as ramp-rate limits of the diesel engines at specified load levels and practical battery SOC limits. In addition, the algorithm is designed to reduce the transient power on the engines and consequently, the mechanical wear can be minimized by assigning the transient loads to the batteries.

II. Case Study Vessel and Load Profile

The target vessel for the EMS study is determined as offshore support vessels (OSVs), especially for platform supply vessels (PSV) and specialized offshore vessels (SOV). OSVs are operated to transport personnel and supplies/equipment and perform service operations, sailing between offshore platforms/wind turbines and shore facilities. Therefore, these vessels show different types of operation scenarios from harboring mode near/at the port to dynamic positioning (DP) mode near/at the platform. In harboring mode, the power system runs at a very low load since only the hotel loads from the accommodation block are online. However, in DP mode, high load fluctuations can be expected in the power system depending on the environmental conditions such as wind, waves, and currents.

In Fig. 2, a typical load profile of an OSV is presented, and this load profile is used as the basis for further optimization. The selected total duration of the power measurement is approximately 35 hours and each data sampling interval is 5 seconds.

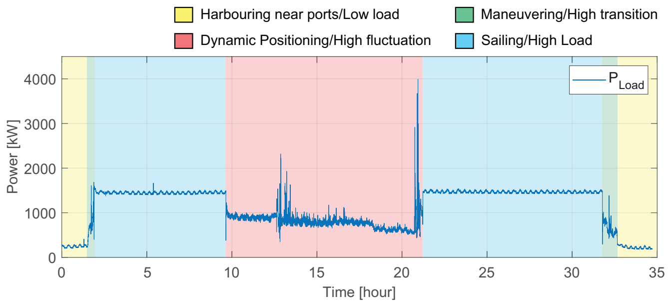

Fig. 2: Typical load profile of offshore support vessels

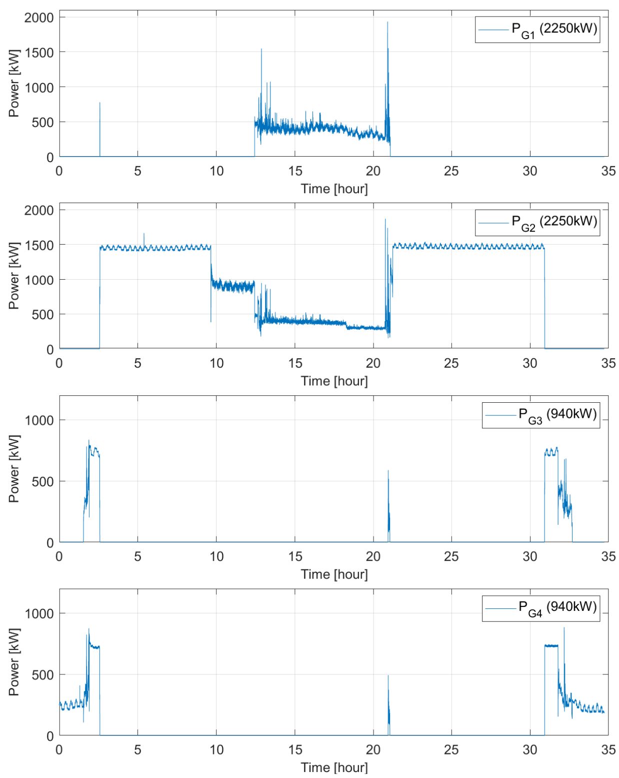

Fig. 3: Original Scheduling of the power plant in the OSV

The operation scenario is symmetrical because the OSV has a round trip between the platform and shore. The vessel starts to operate in harboring mode with a very low load before the sailing starts. Then, the diesel generators must be operating at a very low load with lower fuel efficiency. This operation point can be a good candidate to reduce the fuel consumption by the ESS. Then, the OSV sails to the open sea by maneuvering and ramp-up operation where the load increases with some fluctuations that can be later minimized by the ESS. On the open sea, the OSV can finally sail to the platform at high-speed. When the OSV arrives at/near the platform, it must keep its position to secure the cargo handling operation with deck machinery such as cranes. DP operation and cargo handling operation cause the highest fluctuations in the power system as seen in Fig. 2, so the ESS should be utilized in a way to minimize the fluctuations. Afterward, the OSV sails back to the shore.

From the load profile analysis, it can be observed how the ESS can contribute to better fuel efficiency and power system stability. For example, the ESS enables to run one large and one small generator or two small generators in DP mode instead of two large generators. Without the ESS, the operation of a small generator might be risky to take the high transient load. Furthermore, scheduling of the power sources can minimize the running hours of each generator for reduced maintenance costs. Hereafter, a battery system is considered for ESS. Battery systems are the most viable solution because they have been widely adopted in marine applications, showing continuously improved safety and reduced installation cost.

As a benchmark, the target OSV has four diesel generator sets (genset), two big gensets of 2250 kW (G1 and G2) and two small gensets of 940 kW (G3 and G4). Based on the load profile given in Fig. 2, the original scheduling of the power plant is presented in Fig. 3.

The big gensets are used during high-speed sailing and DP conditions while the small gensets are used in low-load and maneuvering operations. However, during DP mode, the small gensets should be connected to the grid in idle mode to support the power system in case of very high transient conditions such as at 21 hour. As expected earlier, the high transient loads are absorbed by the diesel engines. This can cause a highly fluctuating shaft speed which results in AC frequency instability and poor combustion/fuel efficiency with increased emissions due to the turbo-lag in the engine auxiliary systems.

The proposed EMS aims to carry out an improved power plant scheduling with the battery operation. The EMS calculates a slow-varying power reference for the gensets and separates the transient load. Then, the transient load is assigned to the battery, so the gensets are not necessary to absorb high transient loads, thus achieving increased energy efficiency. At the same time, the algorithm allocates the load level of the genset to a more efficient level so that the fuel consumption of the power plant can be further decreased.

III. Development of Energy Management System

In this section, the development of the proposed EMS is presented including the objective function and the constraints of the optimization algorithm.

A. MILP formulation of the Specific Fuel Consumption

Due to the limitation of SFC data for the small engines as shown in Fig. 4(a), and for big engines as shown in Fig. 4(b), a quadratic function is used to estimate additional SFC data points at every five load percent. Therefore, it is assumed that a total of 21 measured SFC points are available for each engine type. Then, the obtained SFC data is formulated with MILP form to calculate fuel consumption as presented in Fig. 4(c) for small engines and in Fig. 4(d) for big engines. Among the piecewise linearization method, the convex combination (CC) method is chosen to be more accurate in the selection of the load percent. Then, the MILP algorithm chooses a load percent by selecting one region with $z_{i,j}$ as a binary variable

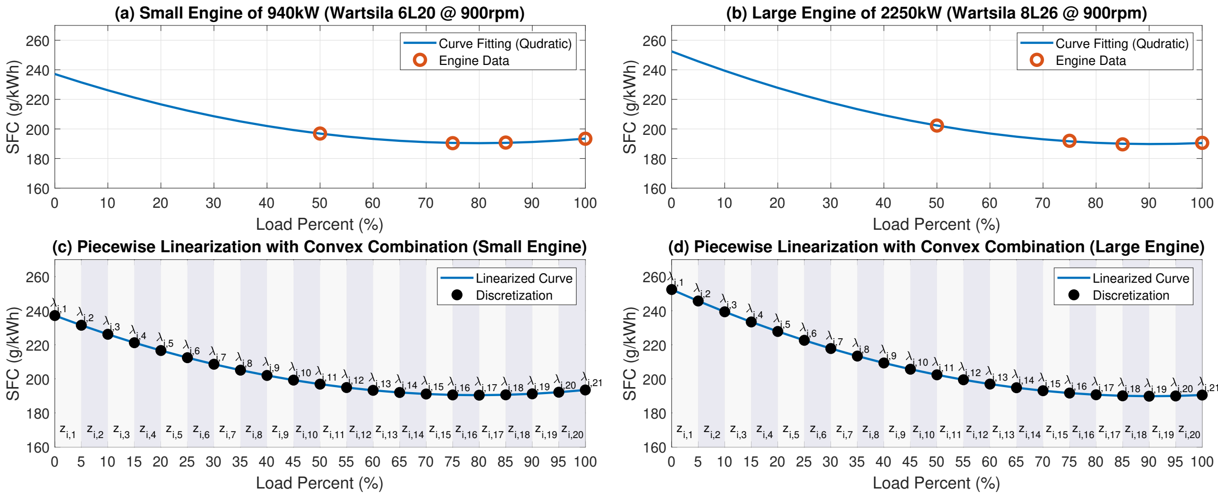

Fig. 4: Curve fitting and piecewise linearization with convex combination for specific fuel consumption ($SFC_{i,j}$) of diesel engines (Courtesy of Wärtsilä)

and calculates internally dividing points between the adjoining $\lambda_{i,j}$ and $\lambda_{i,j+1}$ as continuous variables with a range between 0 and 1, where i represents the i-th engine and j represents the j-th region of the SFC. For example, if $z_{i,6} = 1$ and $\lambda_{i,6} = \lambda_{i,7} = 0.5$, the selected load percent becomes 27.5 %.

B. Goal Programming: Linearization of Absolute Value Functions

If an absolute value function is used in the objective function for the penalization of certain deviations, this will violate the LP-formulation. Without the absolute function, the algorithm chooses the infinite negative deviation, so the resulting solutions are not correct. Therefore, to solve this problem, the goal programming approach is used to replace the absolute value functions.

When the distance between a reference value x_{ref} and a variable x should be calculated as $|x_{ref} - x|$, this can be re-written as:

$$|x_{ref} - x| = \text{ minimize } (w^+ d^+ + w^- d^-) \tag{1}$$

$$\text{s.t. } x_{ref} - x = d^+ - d^- \tag{2}$$

$$\text{where } d^+, d^- \geq 0 \tag{3}$$

where d^+, d^- are the distance variables and w^+ and w^- are the weighting factors (chosen as 1 hereafter). Since $d^+ + d^-$ should be minimized by including this term in the objective function, either d^+ or d^- becomes eventually zero depending on the negative or positive distance in each case. For example, if $|x_{ref} - x| = |0 - 1| = 1$, $d^+ = 0$ and $d^- = 1$ so that $x_{ref} - x = d^+ - d^- = -1$ and $d^+ + d^- = 1$.

Before describing the optimization function, the decision variables are explained in Table. I and the indexes and parameters are listed in Table II.

C. Objective Function

In this section, the objective function is defined with the formulation techniques explained above as:

$$\text{minimize} \quad \underbrace{C(P_{g,i})[k]}_{\text{Equivalent fuel cost function of the gensets}} \tag{4}$$

$$+ \underbrace{\omega_{g,num} \cdot \sum_{i=1}^{4} \lambda_{g,i}[k]}_{\text{minimization of operating number of gensets}} \tag{5}$$

$$+ \underbrace{\omega_{g,rp} \cdot \sum_{i=1}^{4} (d_{gr}^{+} + d_{gr}^{-})}_{\text{Penalizing for steep load change of the gensets}} \tag{6}$$

$$+ \underbrace{\omega_{b,soc} \cdot (d_{gb}^{+} + d_{gb}^{-})}_{\text{Penalizing for low battery SOC}} \tag{7}$$

$$+ \underbrace{\omega_{rp,slack} \cdot \gamma_i}_{\text{Penalizing for relaxing ramp limit}} \tag{8}$$

In Eq. (4), based on the selected load percentage with j for each genset i, the total fuel consumption multiplied by weighting factors will be calculated during the time interval Δt in [ton] unit. The detailed calculation for the fuel consumption is formulated as an equality constraint in Eq. (9) and Eq. (10). The terms from the second to the last term of the objective function are penalizing functions.

To penalize the battery SOC, rule-based reference values of SOC_{ref} are defined. Depending on the operation mode, SOC_{ref} can be adjusted to reflect the higher possibility of the intended charge or discharge strategy of the battery. For example, in low-load conditions, SOC_{ref} is set to 0.8 to charge the battery as much as possible and SOC_{ref} is set to 0.2 during the high transient conditions to adsorb varying loads. Also, SOC_{ref} is set to 0.2 at the end of the sailing trip in order to fully utilize the battery before the shore-charging.

TABLE I: Nomenclature - Decision Variables

Variables	
$\lambda_{g,i}$	Start/stop of the gensets, $\lambda_{g,i} \in \{0,1\}$
$\lambda_{i,j}$	Gensets load selector for piecewise linearization
$z_{i,j}$	Gensets load selector for piecewise linearization with convex combination, $z_{i,j} \in \{0,1\}$
$P_{g,i}$	Power of the gensets at each load percent
P_{bat}	Power of the battery
SOC	State of charge of the battery (dependent on P_{bat})
d^+_{gr}, d^-_{gr}	Distance variables for $P_{g,i}[k] - P_{g,i}[k-1]$
d^+_{gb}, d^-_{gb}	Distance variables for $SOC[k] - SOC_{ref}[k]$
γ_i	Slack variable to relax the ramp limit, $\gamma_i \in \{0,1\}$

TABLE II: Nomenclature - Indexes and Parameters

Indexes	
k	Time instance
i	Identification number of the gensets (i = 1, 2, 3, 4)
j	Discretized load percent of the gensets
Parameters	
$N_{g,min}$	The minimum number of operating gensets
$N_{g,max}$	The maximum number of operating gensets
N_{Lp}	Total number of discretized load percent
$P_{g,rated,i}$	Rated power of the gensets (2250 kW and 940 kW)
P_{rp}	Ramp limit as defined in Fig. 5
$P_{g,rp,h,i}$	Limit of the load increase (Load $\geq$ 50 %)
$P_{g,rp,l,i}$	Limit of the load increase (Load $<$ 50 %)
$P_{g,rp,rlx,i}$	Allowable increase of ramp rate for each genset in case of constraint relaxation
$SFC_{i,j}$	SFC of each genset at a given load percent
$fuel_{g,i}$	Fuel consumption of each genset during a given interval
P_{load}	Total load of the consumers
$P_{load,ft}$	Filtered total load of the consumers
SOC_0	Initial state of charge at each iteration ($SOC_0 = 0.9$)
SOC_l	SOC lower bound
SOC_u	SOC upper bound
SOC_{ref}	Designated SOC level of the battery
Q_{bat}	Capacity of the battery
$P_{bat,ch}$	Charging power limit of the battery
$P_{bat,disc}$	Discharging power limit of the battery
Δt	Time interval that each optimization holds
Parameters: Weighting factors	
$\omega_{g,fc,i}$	Penalizing each genset's fuel consumption
$\omega_{g,num}$	Penalizing the number of operating gensets
$\omega_{g,rp}$	Penalizing the steep load change of gensets
$\omega_{b,soc}$	Penalizing the SOC deviation from its reference
$\omega_{rp,slack}$	Penalizing the slack variable for ramp limit relaxation

A slack variable term in Eq. (8) will relax the constraint of the ramp-up limit of the genset up to the maximum ramp-up capacity by assigning $\gamma_i = 1$ only if the optimization problem becomes infeasible, especially when the load changes too fast above the ramp-up limit and the battery SOC is already too low. As a result, the ramp-up constraint in Eq. (13) will be updated. However, the relaxation of the ramp-up limit should be avoided as much as possible, so the weighting value of $\omega_{rp,slack}$ should be chosen high enough.

D. Equality and Inequality Constraints

In this section, the equality and inequality constraints of the optimization problem are explained. First, the constraints for the gensets are formulated as follows:

$$C(P_{g,i})[k] = \sum_{i=1}^{4}(\omega_{g,fc,i} \cdot fuel_{g,i}(P_{g,i})) \tag{9}$$

$$fuel_{g,i} = \frac{\Delta t}{3600}\sum_{j=1}^{N_{Lp}}(\lambda_{i,j} \cdot P_{g,rated,i} \cdot \frac{j}{100} \cdot \frac{SFC_{i,j}}{1000}) \tag{10}$$

$$0 \leq P_{g,i} \leq \lambda_{g,i} P_{g,rated,i} \tag{11}$$

$$N_{g,min} \leq \sum_{i=1}^{4}\lambda_{g,i} \leq N_{g,max} \tag{12}$$

$$P_{g,i}[k] - P_{g,i}[k-1] \leq P_{rp} + P_{g,rp,rlx,i} \cdot \gamma_i \tag{13}$$

$$P_{rp} = (1 + sign(P_{g,i}[k] - \frac{P_{g,rated,i}}{2})) \cdot \frac{P_{g,rp,h,i}}{2} + (1 + sign(\frac{P_{g,rated,i}}{2} - P_{g,i}[k])) \cdot \frac{P_{g,rp,l,i}}{2} \tag{14}$$

As explained earlier, the fuel consumption calculation is carried out in Eq. (9) and Eq. (10). For choosing a good weighting factor $\omega_{g,fc,i}$, one of the gensets between the same power rating should have a slightly higher weighting factor than the other to avoid switching operations between the same type of gensets. Eq. (11) sets the limitation of the lowest and highest output power from each genset, Eq. (12) defines the limit of the operating number of genset together with the penalizing term in the objective function. $N_{g,max}$ is also defined in a rule-based manner such that a lower number of running gensets is preferred at low-load conditions. Eq. (13) is the ramp-up limit that is calculated based on Eq. (14) depending on the load level of each genset as shown in Fig. 5. The ramp-up limit calculation is based on the operational recommendations of the engine manufacturer and the limitations of the governor.

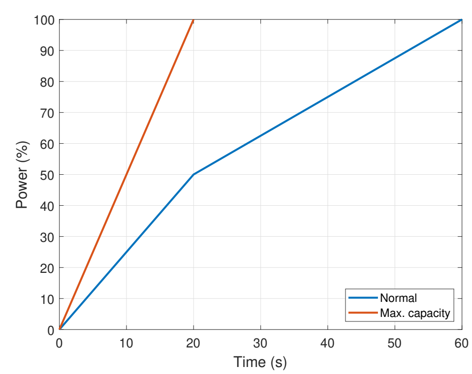

Fig. 5: Ramp limit of the gensets (courtesy of Wärtsilä)

In normal operation, the ramp-up limit follows the blue-line in Fig. 5. If a constraint relaxation is needed, the emergency ramp-up limit as defined by the red line will be used by $P_{g,ramp,rlx,i}$ in Eq. (13). In this case, the slack variable γ_i is selected as 1. In Eq. (15), an equality constraint for the load balance between the power source and the consumer is established. This condition can be also relaxed (optionally) by changing it to an inequality constraint, but, in that case, the main bus voltage should be sacrificed with voltage rise or sag.

$$\sum_{i=1}^{4} P_{g,i} + P_{bat} = P_{load} \tag{15}$$

The equations (16) to (21) represent the piecewise linearization with the convex combination method in MILP formulation.

$$\sum_{j=1}^{N_{Lp}} \lambda_{i,j} = 1 \tag{16}$$

$$\sum_{j=1}^{N_{Lp}-1} z_{i,j} = 1 \tag{17}$$

$$\lambda_{i,j} \geq 0 \tag{18}$$

$$\lambda_{i,1} \leq z_{i,1} \tag{19}$$

$$\lambda_{i,N_{Lp}} \leq z_{i,N_{Lp}-1} \tag{20}$$

$$\lambda_{i,j} \leq z_{i,j} + z_{i,j+1}, \textit{ where j=2,3,...,}N_{Lp}\textit{-1} \tag{21}$$

The battery system constraints including the charging and discharging limits (C-rate limitations) in Eq. (22) and the state of charge (SOC) limitation in Eq. (23) based on the SOC calculation in Eq. (24) are given as:

$$-P_{bat,ch} \leq P_{bat} \leq P_{bat,disc} \tag{22}$$

$$SOC_l \leq SOC \leq SOC_u \tag{23}$$

$$SOC[k] = SOC[k-1] - \frac{\Delta t}{3600 \cdot Q_{bat}} \cdot P_{bat} \tag{24}$$

Lastly, the constraints for the linearization of absolute value functions are formulated in equations (25) to (28). It should be noted that the penalizing term for load changes in Eq. (6) and Eq. (27) requires a memory of the previous genset load at the $(k-1)$ time instance.

$$d_{gr}^{+}, d_{gr}^{-} \geq 0 \tag{25}$$

$$d_{gb}^{+}, d_{gb}^{-} \geq 0 \tag{26}$$

$$P_{g,i}[k] - P_{g,i}[k-1] = d_{gr}^{+} - d_{gr}^{-} \tag{27}$$

$$SOC[k] - SOC_{ref}[k] = d_{gb}^{+} - d_{gb}^{-} \tag{28}$$

IV. Results and discussions

The optimization algorithm is implemented in Python using the PuLP framework [17] that works as an interface to IBM CPLEX as a solver. By adopting MILP formulation with Python, it is observed that the calculation time of each iteration is always faster than real-time meaning that from 1.5 to 6 calculations can be done at every second. This ensures that the proposed EMS is able to solve the optimization problem within any sampling time interval higher than 1 s. In this study, the sampling time of the measurements is chosen as 5 s considering the communication delay.

The simulation cases are divided into three different scenarios (Case A, Case B, and Case C). Battery operation is considered in Case B and Case C, but not in Case A. With battery operation, Case B minimizes the fuel consumption with relatively less penalization of transient load to the gensets, while Case C strictly penalizes transient operation and a higher number of operating gensets. The specifications of the power plant in the OSV are described in Table III, and the weighting factors used in each case are listed in Table IV. Comparing the results, the best weighting factors are found by try and error method.

TABLE III: The specifications of the power plant

Parameter	Value
Diesel Generator 1 (G1)	2250 kW
Diesel Generator 2 (G2)	2250 kW
Diesel Generator 3 (G3)	940 kW
Diesel Generator 4 (G4)	940 kW
Battery System	300/600/1000 kWh
Battery C-Rate	3C / 2C (discharging/charging)

TABLE IV: The weighting factors for each simulation case (FC: fuel consumption, MAINT: maintenance)

Weighting Factor	Case A (w/o Battery)	Case B (w/ Battery) (min. FC)	Case C (w/ Battery) (min. MAINT)
$\omega_{g,fc,1}$	20	20	20
$\omega_{g,fc,2}$	20.02	20.02	20.02
$\omega_{g,fc,3}$	20	20	20
$\omega_{g,fc,4}$	20.01	20.01	20.01
$\omega_{g,num}$	0	0	5
$\omega_{g,rp}$	0	0.011	0.1
$\omega_{b,soc}$	0	150	150
$\omega_{rp,slack}$	5	5	5

The results with a battery capacity of 1000 kWh are presented in Fig. 6. The results show that the total fuel consumption is reduced for all cases compared to the original operation scenario. For the Case A, B, and C, a reduction of 5.437 %, 7.187 %, and 1.176 % has been achieved respectively. The results show that a reduction of fuel consumption is possible even without battery operation, but in this case, the gensets must encounter all the load fluctuations as seen in Fig. 6(a). Therefore, by using the battery, both total fuel consumption and the fluctuation can be minimized as seen in Fig. 6(b) and (c). Based on the battery power and SOC for Case B, it is noted that the battery works as a low pass filter for the gensets load. The benefit of using an optimization filter is to obtain guaranteed fuel reduction as well as fluctuation minimization. However, the total running hours of the gensets are slightly increased by 7.1 % compared to the original operation.

In order to minimize the total running hours of the gensets, the weighting factor, $\omega_{g,rp}$ is increased by approximately 10 times. The result in Fig. 6(c) shows that G1 (the bigger genset) and the battery can handle the load by decreasing the total running hours by 23.0 % compared to the original operation. Therefore, G1 is mainly online except that G3 (the smaller genset) should be operated from 2 h to 5 h where the battery has reached its lowest SOC limit (20 %). Besides, in this case, the fuel consumption reduction has to be sacrificed compared to Case B but it is still better than the original operation.

The optimization problem has also been performed for a battery with smaller capacities as all other parameters remained unchanged. The optimization results for the different battery sizes are summarized in Table V and the improvements are indicated in percent compared to the original operation. It is worth mentioning that the original total fuel consumption and

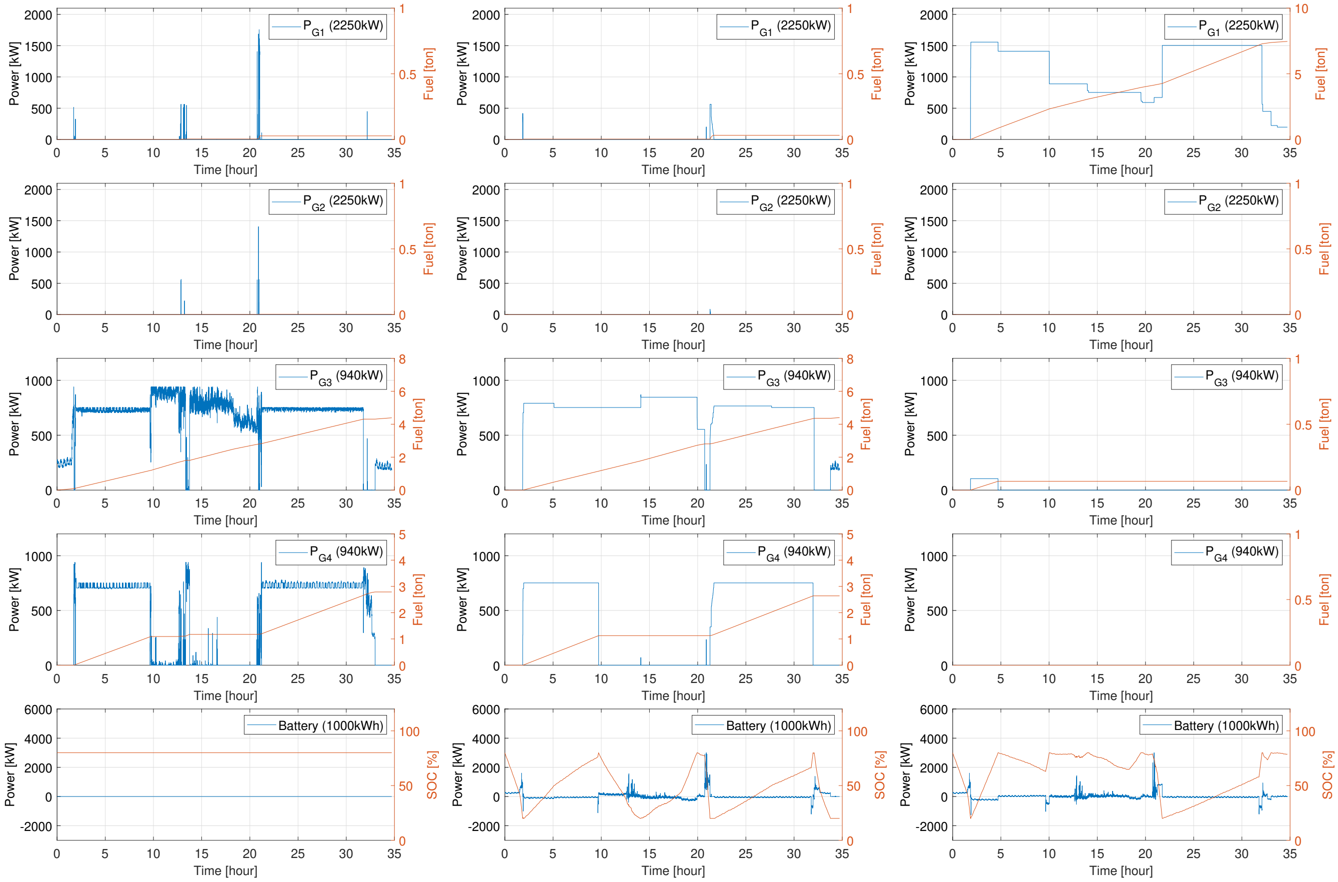

(a) Case A (b) Case B (c) Case C

Fig. 6: Optimization results for different objectives: (a) Case A: without battery and fuel minimization, (b) Case B: with battery and fuel minimization, and (c) Case C: with battery and maintenance minimization.

the total sum of running hours of each genset are 7.622 tonnes and 46.418 hours respectively.

Observing Case B, the results show that increasing the battery size does not necessarily lead to lower fuel consumption as the fuel reduction fluctuates in the battery capacities of 300-600 kWh. In order to achieve significant fuel reduction, the battery capacity should also increase significantly to 1000 kWh. This comparison study can be used for battery dimensioning. For example, if 5 % of the fuel reduction is satisfactory, the battery capacity of 300 kWh becomes the base case. Then, a designer can add more capacity up to 600 kWh to consider battery aging and energy buffer.

Meanwhile, the running hours in Case B are increased compared to the original operation to achieve higher fuel reduction. By compromising the fuel-saving, the running hour can be reduced significantly as seen in Case C. However, the case of 600 kWh shows the least improvement in the running hour since it has higher fuel reduction compared to the other cases. Alternatively, this can be further improved by the tuning of the weighting factors.

In Fig. 7, the results of each case are re-calculated as an averaged specific fuel consumption that can indicate the efficiency of fuel usage with the averaged load percent for each type of engine over the whole period of simulation time. This comparison shows that, based on the given load profile and compared to the original operation profile, higher energy efficiency can be achieved in some cases (lower SFCs than the original SFC) by using the small engines. However, Case B cannot avoid sacrificing the efficiency of the large engines, but the operation time of the large engines is very short. On the contrary to this result, Case C results achieve higher engine efficiency for the large engines because the optimization commands to use one large engine constantly instead of the small engines in order to minimize the running

TABLE V: The summary of the optimization results

	Fuel Reduction			**Running Hour Reduction**		
Battery Capacity	**CaseA**	**CaseB**	**CaseC**	**CaseA**	**CaseB**	**CaseC**
-	5.4%	-	-	-17.9%	-	-
300kWh	-	5.1%	1.1%	-	-27.6%	**26.8%**
600kWh	-	5.3%	2.3%	-	-14.3%	9.8%
1000kWh	-	**7.2%**	1.2%	-	-7.1%	23.0%

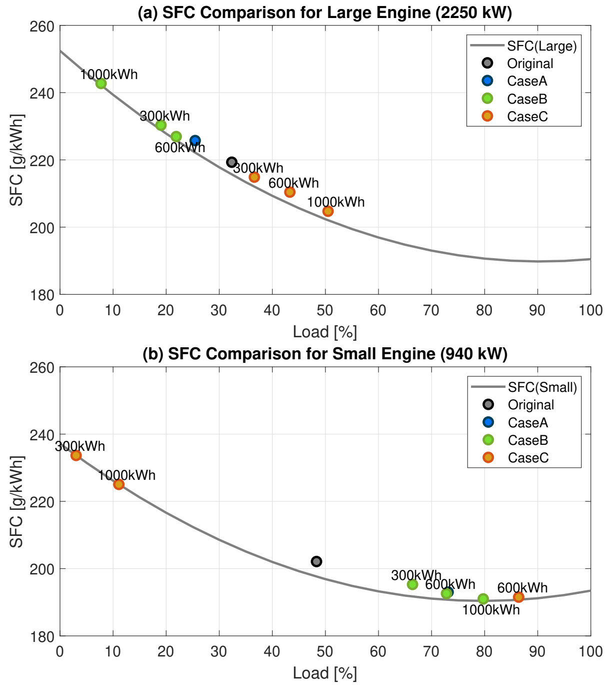

Fig. 7: The comparison of the averaged SFCs based on the different case studies. (a) SFC for large engine type (b) SFC for small engine type

hours of the power plant. To sum up, it is noted that the operation with higher battery capacity has a higher potential to reduce fuel consumption and the running hours in general. However, it should be also noted that the battery cost and payback time should be carefully considered.

V. Conclusion

This paper has proposed an optimal energy management system for hybrid shipboard power systems with engine-generators and batteries. The optimization algorithm for the EMS is based on a MILP formulation considering the physical and technical constraints of the power system. The nonlinear SFC function of the engines is re-formulated with piecewise linearization. The piecewise linearization also makes it easier to update the SFC curve in the algorithm over the life-cycle of the ship. To test and tune the algorithm, the case studies have been performed based on real OSV operation data with different battery sizes: Case A - fuel optimization without battery and only gensets, Case B - fuel optimization with battery, and Case C - optimization of fuel and running hours with battery. While a reduction of fuel consumption has been achieved for all cases, a reduction of running hours of the gensets has been observed for Case C only. It can be assumed that for achieving better fuel efficiency, the running hours are usually compromised in the conventional methods. In this study, the results show that both fuel and running hours' reduction can be achieved by balancing between the two objectives with a proper choice of the battery SOC reference and the tuning parameters. In addition, the algorithm assigns the transient loads to the battery system, so the engine-gensets can be operated with less power transient. This can reduce the frequency fluctuations and mechanical wear of the engines, which can influence the engine-related OPEX.

References

[1] P. Ghimire, D. Park, M. K. Zadeh, J. Thorstensen, and E. Pedersen, "Shipboard Electric Power Conversion: System Architecture, Applications, Control, and Challenges [Technology Leaders]," *IEEE Electrification Mag.*, vol. 7, DOI: 10.1109/MELE.2019.2943948, no. 4, pp. 6–20, Dec. 2019.

[2] L. W. Y. Chua, T. Tjahjowidodo, G. G. L. Seet, and R. Chan, "Implementation of Optimization-Based Power Management for All-Electric Hybrid Vessels," *IEEE Access*, vol. 6, DOI: 10.1109/ACCESS.2018.2883324, pp. 74 339–74 354, 2018.

[3] D. Park and M. Zadeh, "Modeling and predictive control of shipboard hybrid dc power systems," *IEEE Trans. Transport. Electrific*, vol. 7, DOI: 10.1109/TTE.2020.3027184, no. 2, pp. 892–904, 2021.

[4] D. Park and M. Zadeh, "Dynamic modeling, stability analysis and power management of shipboard dc hybrid power systems," *IEEE Trans. Transport. Electrific*, DOI: 10.1109/TTE.2021.3119231, pp. 1–1, 2021.

[5] B. Zahedi, L. E. Norum, and K. B. Ludvigsen, "Optimized efficiency of all-electric ships by dc hybrid power systems," *Journal of Power Sources*, vol. 255, pp. 341–354, Jun. 2014.

[6] E. A. Sciberras, B. Zahawi, D. J. Atkinson, A. Breijs, and J. H. v. Vugt, "Managing Shipboard Energy: A Stochastic Approach Special Issue on Marine Systems Electrification," *IEEE Trans. Transport. Electrific.*, vol. 2, no. 4, Dec. 2016.

[7] M. R. Banaei and R. Alizadeh, "Simulation-Based Modeling and Power Management of All-Electric Ships Based on Renewable Energy Generation Using Model Predictive Control Strategy," *IEEE Intell. Transp. Syst. Mag.*, vol. 8, DOI: 10.1109/MITS.2016.2533960, no. 2, pp. 90–103.

[8] P. Ghimire, M. Zadeh, E. Pedersen, and J. Thorstensen, "Dynamic Modeling, Simulation, and Testing of a Marine DC Hybrid Power System," *IEEE Trans. Transp. Electrification*, vol. 7, DOI: 10.1109/TTE.2020.3023896, no. 2, pp. 905–919.

[9] L. Thorat and R. Skjetne, "Optimal Online Configuration and Load-Sharing in a Redundant Electric Power System for an Offshore Vessel Using Mixed Integer Linear Programming," in *OMAE2018*, DOI: 10.1115/OMAE2018-77955.

[10] H. Grimmelius, P. de Vos, M. Krijgsman, and E. van Deursen, "Control of hybrid ship drive systems," in *Proc. 10th Int. Conf. Comput. IT Appl. Maritime Ind*, pp. 1–15, Berlin, 2011.

[11] E. Skjong, T. A. Johansen, M. Molinas, and A. J. Sørensen, "Approaches to Economic Energy Management in Diesel–Electric Marine Vessels," *IEEE Trans. Transp. Electrification*, vol. 3, DOI: 10.1109/TTE.2017.2648178, no. 1, pp. 22–35, Mar. 2017.

[12] A. Boveri, F. Silvestro, M. Molinas, and E. Skjong, "Optimal Sizing of Energy Storage Systems for Shipboard Applications," *IEEE Trans. Energy Convers.*, vol. 34, DOI: 10.1109/TEC.2018.2882147, no. 2, pp. 801–811, Jun. 2019.

[13] M. Kalikatzarakis, R. D. Geertsma, E. J. Boonen, K. Visser, and R. R. Negenborn, "Ship energy management for hybrid propulsion and power supply with shore charging," *Control Engineering Practice*, vol. 76, DOI: 10.1016/j.conengprac.2018.04.009, pp. 133–154, Jul. 2018.

[14] A. Boveri, P. Gualeni, D. Neroni, and F. Silvestro, "Stochastic approach for power generation optimal design and scheduling on ships," in *2017 IEEE PES Innovative Smart Grid Technologies Conference Europe (ISGT-Europe)*, DOI: 10.1109/ISGTEurope.2017.8260334, pp. 1–6, Sep. 2017.

[15] H. Park, J. Sun, S. Pekarek, P. Stone, D. Opila, R. Meyer, I. Kolmanovsky, and R. DeCarlo, "Real-Time Model Predictive Control for Shipboard Power Management Using the IPA-SQP Approach," *IEEE Trans. Control Syst. Technol.*, vol. 23, DOI: 10.1109/TCST.2015.2402233, no. 6, pp. 2129–2143, Nov. 2015.

[16] P. Xie, J. M. Guerrero, S. Tan, N. Bazmohammadi, J. C. Vasquez, M. Mehrzadi, and Y. Al-Turki, "Optimization-Based Power and Energy Management System in Shipboard Microgrid: A Review," *IEEE Syst. J.*, pp. 1–13, 2021.

[17] S. Mitchell, S. M. Consulting, and I. Dunning, "Pulp: A linear programming toolkit for python," 2011.